

See discussions, stats, and author profiles for this publication at: <https://www.researchgate.net/publication/350098926>

# Shed the light on virus: virucidal effects of 405 nm visible light on SARS-CoV-2 and influenza A virus. 2

Preprint · March 2021

CITATIONS

0

READS

15

6 authors, including:



**Raveen Rathnasinghe**

Icahn School of Medicine at Mount Sinai

23 PUBLICATIONS 249 CITATIONS

SEE PROFILE



**Sonia Jangra**

Icahn School of Medicine at Mount Sinai

11 PUBLICATIONS 28 CITATIONS

SEE PROFILE



**Lisa Miorin**

Icahn School of Medicine at Mount Sinai

41 PUBLICATIONS 3,622 CITATIONS

SEE PROFILE

Some of the authors of this publication are also working on these related projects:



Flavivirus molecular virology [View project](#)



Towards a live attenuated universal Influenza vaccine (LAIV): The use of  $\Delta$ NS1 viruses as a platform [View project](#)

1 **Shed the light on virus: virucidal effects of 405 nm visible light on SARS-CoV-2**  
2 **and influenza A virus.**

3 Raveen Rathnasinghe<sup>1,2,3</sup>, Sonia Jangra<sup>1,2</sup>, Lisa Miorin<sup>1,2</sup>, Michael Schotsasert<sup>1,2</sup>, Clifford  
4 Yahnke<sup>6#</sup>, Adolfo García-Sastre<sup>1,2,4,5#1</sup>

5 <sup>1</sup>Department of Microbiology, Icahn School of Medicine at Mount Sinai, New York, NY 10029, USA

6 <sup>2</sup>Global Health and Emerging Pathogens Institute, Icahn School of Medicine at Mount Sinai, New York,  
7 NY 10029, USA

8 <sup>3</sup>Graduate School of Biomedical Sciences, Icahn School of Medicine at Mount Sinai, New York, NY  
9 10029, USA

10 <sup>4</sup>Department of Medicine, Division of Infectious Diseases, Icahn School of Medicine at Mount Sinai, New  
11 York, NY 10029, USA

12 <sup>5</sup>The Tisch Cancer Institute, Icahn School of Medicine at Mount Sinai, New York, NY 10029, USA

13 <sup>6</sup> Kenall Manufacturing, Kenosha, WI 53144

14 #Correspondence: [cliff.yahnke@kenall.com](mailto:cliff.yahnke@kenall.com) , [adolfo.garcia-sastre@mssm.edu](mailto:adolfo.garcia-sastre@mssm.edu)

15 **Abstract**

16 Germicidal potential of specific wavelengths within the electromagnetic spectrum is an  
17 area of growing interest. While ultra-violet (UV) based technologies have shown  
18 satisfactory virucidal potential, the photo-toxicity in humans coupled with UV associated  
19 polymer degradation limit its use in occupied spaces. Alternatively, longer wavelengths  
20 with less irradiation energy such as visible light (405 nm) have largely been explored in  
21 the context of bactericidal and fungicidal applications. Such studies indicated that 405  
22 nm mediated inactivation is caused by the absorbance of porphyrins within the  
23 organism creating reactive oxygen species which result in free radical damage to its  
24 DNA and disruption of cellular functions. The virucidal potential of visible-light based  
25 technologies has been largely unexplored and speculated to be not effective given the  
26 lack of porphyrins in viruses. The current study demonstrated increased susceptibility of

27 lipid-enveloped respiratory pathogens of importance such as SARS-CoV-2 (causative  
28 agent of COVID-19) as well as the influenza A virus to 405nm, visible light in the  
29 absence of exogenous photosensitizers, indicating a potential porphyrin-independent  
30 alternative mechanism of visible light mediated viral inactivation. Given that visible light  
31 is generally safe to humans, our results support further exploration of the use of visible  
32 light technology for the application of continuous decontamination in areas within  
33 hospitals and/or infectious disease laboratories, specifically for the inactivation of  
34 respiratory pathogens such as SARS-CoV-2 and Influenza A.

35 **Key words – Visible light, 405nm, Virucidal, SARS-CoV-2, Influenza, inactivation**

36

37

38

39

40

41

42

43

44

45

46

47

## 48 **Introduction**

49 The severe-acute respiratory syndrome corona virus 2 (SARS-CoV-2), the causative  
50 agent of the COVID-19 pandemic, is a member of the beta-coronavirus family and it  
51 emerged at the end of 2019 in the Hubei province in Wuhan China<sup>1</sup>. By late February  
52 2021, more than 112 million cases had been reported while accounting for  
53 approximately 2.5 million deaths, underscoring the rapid dissemination of the virus on a  
54 global scale<sup>2</sup>. As a complement to standard precautions such as handwashing,  
55 masking, surface disinfection, and social distancing, other enhancements to enclosed  
56 spaces such as improved ventilation and whole-room disinfection are being considered  
57 by segments beyond acute healthcare such as retail, dining, and transportation<sup>3</sup>.

58 Initial guidance from health authorities such as the CDC and WHO on environmental  
59 transmission focused on contaminated surfaces as fomites<sup>4</sup>. Data pertaining to the  
60 survival of SARS-CoV-2 and other related coronaviruses to date has indicated that  
61 virions are able to persist on fomites composed of plastic<sup>5</sup>, wood<sup>6</sup>, paper<sup>5</sup>, metal<sup>7</sup> and  
62 glass<sup>8</sup> potentially up to nine days. Recent studies have suggested that SARS-CoV-2  
63 may also remain viable approximately at least three days in such surfaces and another  
64 two studies showed that at room temperature (20-25°C), a 14-day time-period was  
65 required to see a 4.5-5 Log<sub>10</sub> of the virus<sup>9, 10</sup>.

66 Since the start of the pandemic, transmission of the virus by respiratory droplets and  
67 aerosols has become an accepted method of transmission although the relative impact  
68 of each mode of transmission is the subject of much debate. Nevertheless, enclosed

69 spaces with groups of people exercising or singing have been associated with  
70 increased transmission. The half-life survival of SARS-CoV-2 in this type of  
71 environment has been estimated between 1-2 hours<sup>6, 11, 12</sup>.

72 Taking this information into consideration, several methods have been evaluated to  
73 effectively inactivate SARS-CoV-2. Chemical methods, which focus on surface  
74 disinfection, utilize 70% alcohol and bleach and their benefits are well established.  
75 These methods are also episodic (or non-continuous) meaning that in-between  
76 applications, the environment is not being treated<sup>13</sup>.

77 In addition to chemicals, one of the most utilized methods for whole-room disinfection is  
78 germicidal ultra-violet C (UVC; ~254 nm)<sup>14</sup>. This technology is well established<sup>15</sup> and  
79 has been shown to inactivate a range of pathogens including bacteria<sup>16</sup>, fungi<sup>17</sup> and  
80 viruses<sup>18</sup>. The mechanism of action of UVC is photodimerization of genetic material  
81 such as RNA (relevant for SARS-CoV2 and IAV) and DNA (relevant for DNA viruses  
82 and bacterial pathogens, among others)<sup>19</sup>. Unfortunately, this effect has been  
83 associated with deleterious effects in exposed humans such as photokeratoconjunctivitis  
84 in eyes and photodermatitis in skin<sup>20</sup>. For these reasons, UVC irradiation requires safety  
85 precautions and cannot be used to decontaminate fomites and high contact areas in the  
86 presence of humans<sup>21</sup>.

87 Germicidal properties of violet-blue visible light (380-500 nm), especially within the  
88 range of 405 to 450 nm wavelengths have been appreciated as an alternative to UVC  
89 irradiation in whole-room disinfection scenarios where it has shown reduction of  
90 bacteria<sup>22, 23</sup> in occupied rooms and reductions in surgical site infections<sup>24</sup>. Although 405  
91 nm or closely related wavelengths have been shown to be less germicidal than UVC, its

92 inactivation potential has been assessed in pathogenic bacteria such as *Listeria* spp  
93 and *Clostridium* spp<sup>24, 25</sup>, and in fungal species such as *Saccharomyces* spp and  
94 *Candida* spp<sup>26</sup>. It is thought that the underlying mechanism of blue-light mediated  
95 inactivation is associated with absorption of light via photosensitizers such as  
96 porphyrins which results in the release of reactive oxygen species (ROS)<sup>27, 28</sup>. The  
97 emergence of ROS is associated with direct damage to biomolecules such as proteins,  
98 lipids and nucleic acids which are essential constituents of bacteria, fungi and viruses.  
99 Further studies have shown that ROS can also lead to the loss of cell membrane  
100 permeability mediated by lipid oxidation<sup>29</sup>. Given the lack of endogenous  
101 photosensitizers such as porphyrins in virions, efficient decontamination of viruses (both  
102 enveloped and non-enveloped) may require the addition of exogenous  
103 photosensitizers<sup>23</sup>. With the use of media suspensions containing both endogenous  
104 and/or exogenous photosensitizers, inactivation of viruses such as feline calicivirus  
105 (FCV)<sup>30</sup>, viral hemorrhagic septicemia virus (VHSV)<sup>31</sup> and murine norovirus-1<sup>32</sup> has  
106 demonstrated the virucidal potency of 405 nm visible light. Of note, most studies virus  
107 inactivation studies have been performed in media containing porphyrins. In the current  
108 study, we show the impact of 405 nm irradiation on inactivation of SARS-CoV-2 and  
109 influenza A H1N1 viruses without the use of photosensitizers, supporting the possible  
110 use of 405 nm irradiation as a tool to confer continuous decontamination of respiratory  
111 pathogens such as SARS-CoV-2 and influenza A viruses. We further show the  
112 increased susceptibility of lipid-enveloped viruses for irradiation in comparison to non-  
113 enveloped viruses, further characterizing the virucidal effects of visible light.

## 114 **Materials and methods.**

## 115 **405 nm Exposure System**

116 The visible light disinfection product used in this study was Indigo-Clean from Kenall  
117 Manufacturing. The product form factor selected was a 6" downlight (M4DLIC6) to allow  
118 for use within a BSL-3 rated containment hood. Within the hood, the distance between  
119 the face of the fixture and the sample was 10"- much less than the normal 1.5m used in  
120 normal, whole-room disinfection applications. The output of the fixture was modified  
121 electronically during its manufacture to match this difference and ensure that the  
122 measurements would represent the performance of the device in actual use. For the  
123 range of output used in this study, multiple discrete levels were created using pulse  
124 width modulation within the LED driver itself. These levels were made to be individually  
125 selectable using a simple knob on the attached control module.

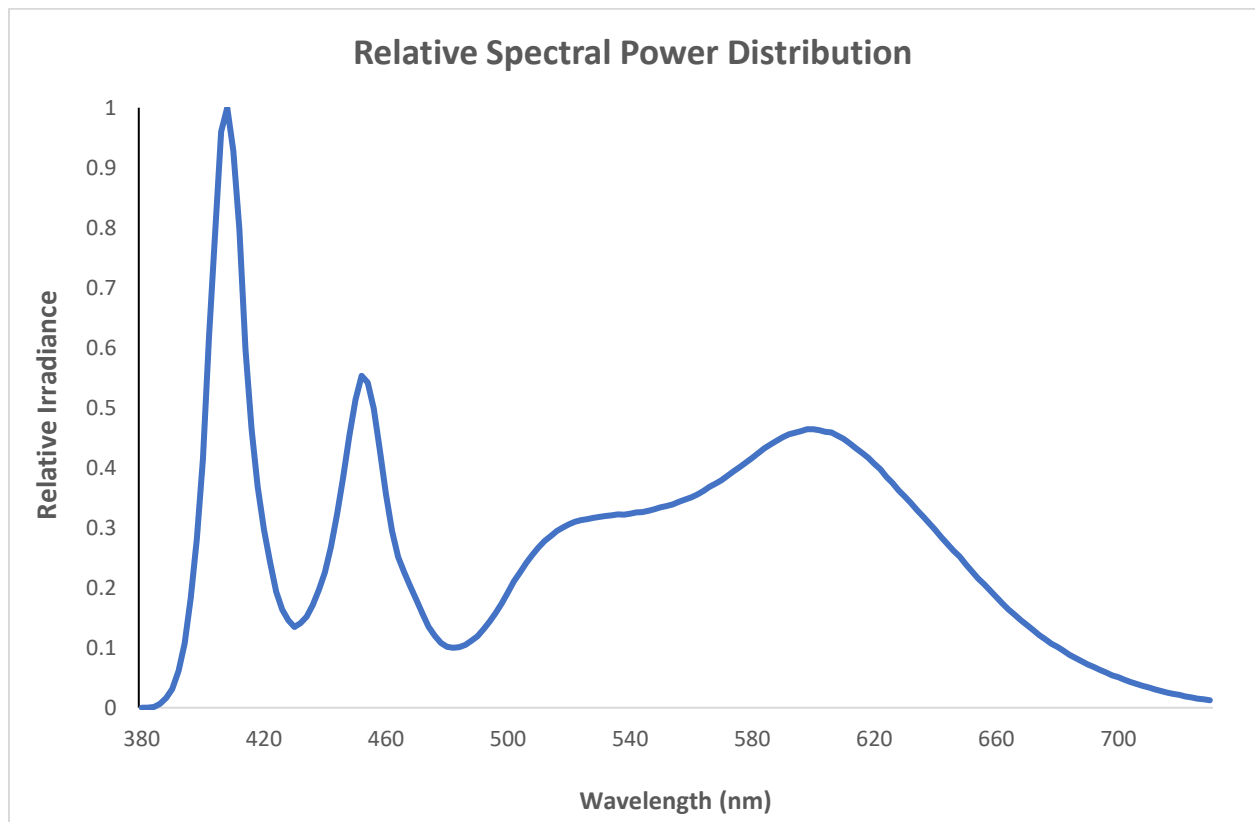
126 As expected, the amount of visible light within the 400nm-420nm bandwidth is a  
127 measurement of the "dose" delivered to the target organism, measured in  $\text{mWcm}^{-2}$ , is  
128 used to quantify this relationship similar to that used in UV disinfection applications.

129 To fully examine this effect, a range of irradiance values were used representing actual  
130 product deployment conditions in occupied rooms. The lowest value ( $0.035 \text{ mWcm}^{-2}$ )  
131 represents a single-mode, lower wattage used in general lighting applications while the  
132 highest value ( $0.6 \text{ mWcm}^{-2}$ ) represents a dual-mode, higher wattage used in critical care  
133 applications such as an operating room.

134 The device was placed in a rig to ensure a consistent distance (10") between the fixture  
135 and the samples. The output of the fixture in the test rig was measured using a Stellar-  
136 RAD Radiometer from StellarNet configured to make wavelength and irradiance

137 measurements from 350nm-1100nm with < 1nm spectral bandwidth using a NIST  
138 traceable calibration. To ensure that the regular white light portion of the illumination  
139 (which is non-disinfecting) was not measured, the measurement was electronically  
140 limited to a 1nm bandwidth over the 400nm-420nm range. The normalized spectral  
141 profile is shown in Fig. 1 below. The absolute value of the measurement was  
142 determined using a NIST traceable calibration as previously described.

143



144

145 **Figure 1. Normalized spectral power distribution for Indigo-Clean M4DLIC6**  
146 **showing peak irradiance at 405nm.**

147



148 **Cells and viruses**

149 Vero-E6 cells (ATCC® CRL-1586™, clone E6) were maintained in Dulbecco's Modified  
150 Eagle Medium (DMEM) complemented with 10% heat-inactivated Fetal Bovine Serum  
151 (HI-FBS; PEAK serum), penicillin-streptomycin (Gibco; 15140-122), HEPES buffer  
152 (Gibco; 15630-080) and MEM non-essential amino-acids (Gibco; 25025CL) at 37°C with  
153 5% CO<sub>2</sub>. Vero-CCL81 (ATCC® CRL-81™) cells and MDCK cells (ATCC® CCL-34)  
154 were cultured in DMEM supplemented with 10% HI-FBS and penicillin/streptomycin at -  
155 37°C with 5% CO<sub>2</sub>. All experiments involving SARS-CoV2 (USA-WA1/202, BEI  
156 resource – NR52281) were conducted within a biosafety-level 3 (BSL3) containment  
157 facility at Icahn school of medicine at Mount Sinai by trained workers upon authorization  
158 of protocols by a biosafety committee. Amplification of SARS-CoV-2 viral stocks was  
159 done in Vero-E6 cell confluent monolayers by using an infection medium composed of  
160 DMEM supplemented with 2% HI-FBS, Non-essential amino acids (NEAA), Hepes and  
161 penicillin-streptomycin at 37°C with 5% CO<sub>2</sub> for 72 hours. Influenza A virus used here  
162 was generated using plasmid based reverse genetics system as previously described<sup>33</sup>.  
163 The backbone used in the study was A/Puerto Rico/8/34/Mount Sinai(H1N1) under the  
164 GenBank accession number AF389122. IAV-PR8 virus was grown and titrated in MDCK  
165 as previously described<sup>33</sup>. As a non-enveloped virus, the cell culture adapted murine  
166 Encephalomyocarditis virus (EMCV; ATCC® VR-12B) was propagated and titrated in  
167 Vero-CCL81 cells with DMEM and 2% HI-FBS and penicillin-streptomycin at 37°C with  
168 5% CO<sub>2</sub> for 48 hours<sup>34</sup>.

169 **405nm inactivation of viruses**

170 The SARS-CoV-2 virus was exclusively handled at the Icahn school of Medicine BSL-3  
171 and studies involving IAV and EMCV were handled in BSL-2 conditions. Indicated PFU  
172 amounts were mixed with sterile 1X PBS and were irradiated in 96 well format cell  
173 culture plates in triplicates. In these studies, A starting dose of  $5 \times 10^5$  PFU for SARS-  
174 CoV-2 and starting doses of  $1 \times 10^5$  PFU for IAV and EMCV were used. The final  
175 volumes for inactivation were 250  $\mu$ l per replicate. The untreated samples were  
176 prepared the same way and were left inside the biosafety cabinet isolated from the  
177 inactivation device at room temperature. The plates were sealed with qPCR plate  
178 transparent seal and an approximate 10% reduction of the intensity was observed due  
179 to the sealing film. The distance from the lamp and the samples was measured to be  
180 10". All samples were extracted at indicated times and were frozen at  $-80^\circ\text{C}$  and were  
181 thawed together for titration via plaque assays.

## 182 **Plaque assays**

183 Confluent monolayers of Vero-E6 cells in 12-well plate format were infected with 10-fold  
184 serially diluted samples in 1X phosphate-buffered saline (PBS) supplemented with  
185 bovine serum albumin (BSA) and penicillin-streptomycin for an hour while gently  
186 shaking the plates every 15 minutes. Afterwards, the inoculum was removed, and the  
187 cells were incubated with an overlay composed of MEM with 2% FBS and 0.05% Oxoid  
188 agar for 72 hours at  $37^\circ\text{C}$  with 5%  $\text{CO}_2$ . The plates were subsequently fixed using 10%  
189 formaldehyde overnight and the formaldehyde was removed along with the overlay.  
190 Fixed monolayers were blocked with 5% milk in Tris-buffered saline with 0.1% tween-20  
191 (TBS-T) for an hour. Afterwards, plates were immunostained using a monoclonal  
192 antibody against SARS-CoV2 nucleoprotein (Creative-Biolabs; NP1C7C7) at a dilution

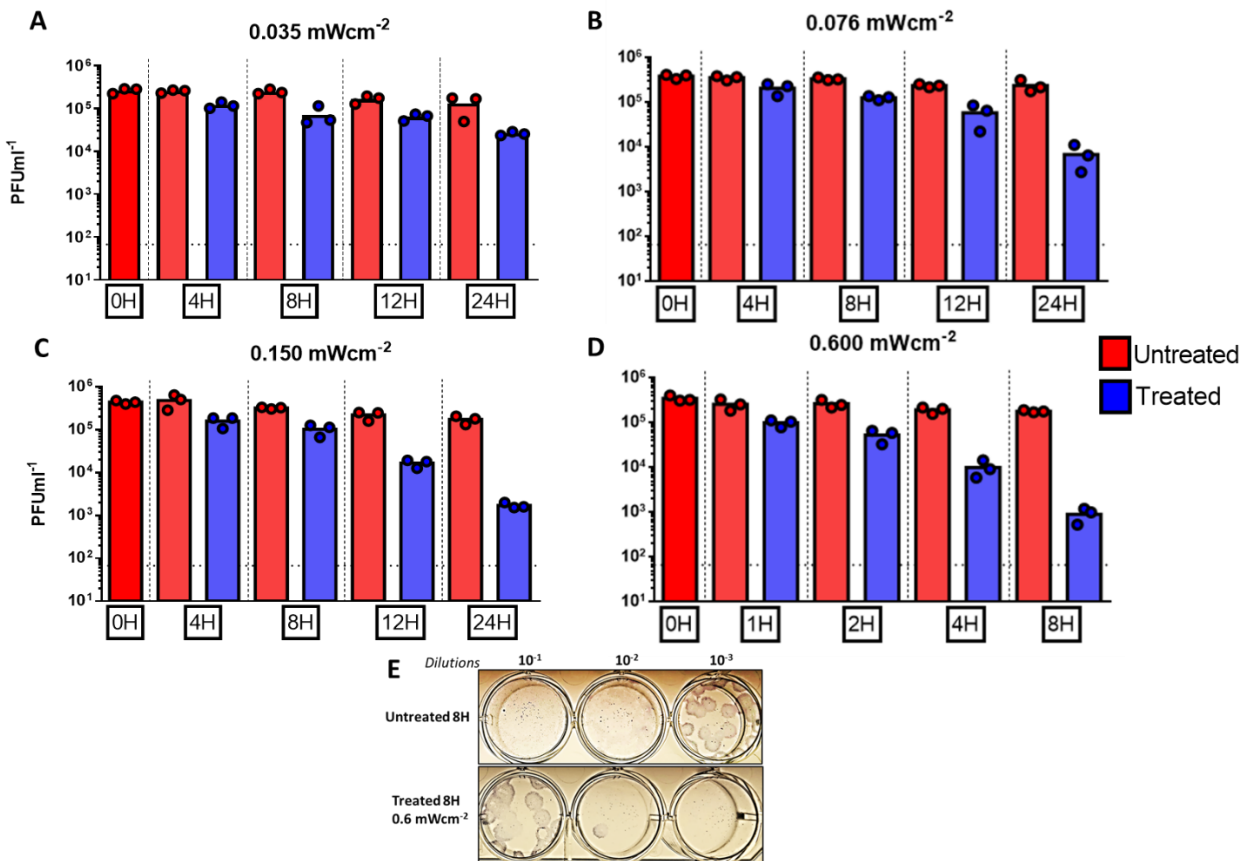
193 of 1:1000 followed by 1:5000 anti-mouse IgG monoclonal antibody and was developed  
194 using KPL TrueBlue peroxidase substrate for 10 minutes (Seracare; 5510-0030). After  
195 washing the plates with distilled water, the number of a plaques were counted. Plaque  
196 assays for IAV and EMCV were done in a similar fashion. For IAV, confluent  
197 monolayers of MDCK cells supplemented with MEM-based overlay with TPCK-treated  
198 trypsin was used. For EMCV, Vero-CCL81 cells were used to do plaque assays in 6  
199 well plate format. Plaques for IAV and EMCV were visualized using crystal violet. Data  
200 shown here is derived from three independent experimental setups.

## 201 **Results.**

### 202 **Dose and time dependent inactivation of SARS-CoV-2 in the absence of** 203 **photosensitizers.**

204 The lowest irradiation dose of  $0.035 \text{ mWcm}^{-2}$  was applied for SARS-CoV-2 and when  
205 compared to the initial input ( $T_0$ ) of  $\sim 5 \times 10^5$  PFU, a reduction of 55.08% was seen as  
206 early as 4 hours and after 24 hours of irradiation, an inactivation of 90.17%  
207 (approximately 10 times reduction in infectivity) was observed for SARS-CoV-2 via  
208 plaque assays (Figure 2A). A slightly higher dose of  $0.076 \text{ mWcm}^{-2}$  resulted in a  
209 reduction of 98.22% (56 times) after 24 hours when compared to the original input at  $T_0$   
210 (Figure 2B). Subsequent increase of the irradiation dose to  $0.150 \text{ mWcm}^{-2}$  resulted in a  
211 reduction of 63.64% after 4 hours which then reached 96.21% after 12 hours. Irradiation  
212 for 24 hours at  $0.150 \text{ mWcm}^{-2}$  suggested a total reduction of 99.61% (256 times) for  
213 SARS-CoV-2 (Figure 2C). As a final experiment, a high irradiation dose of  $0.6 \text{ mWcm}^{-2}$   
214 was used to assess the inactivation potential within a much shorter time frame.  
215 Irradiation for one hour resulted in a reduction of 71.52% which reached 91.15% after

216 four hours and 99.74% (385 times) after 8 hours in comparison to the initial input ( $T_0$ )  
217 (Figure 2 D and E). All experimental conditions demonstrated the stability of untreated  
218 SARS-CoV-2 which was left at room temperature in PBS, as shown by the marginal  
219 reduction of viral titer over time.

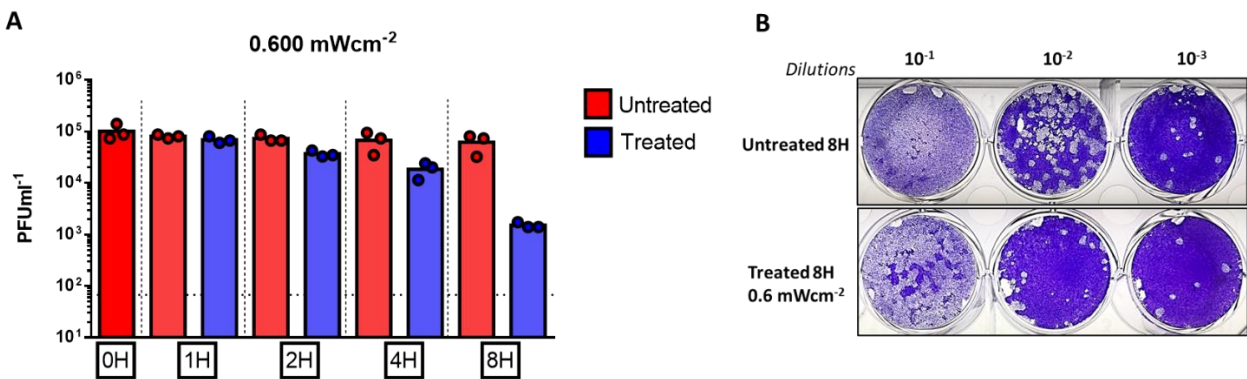


220

221 **Figure 2. Dose and time dependent inactivation of SARS-CoV-2 virus in PBS by 405 nm irradiation.** A. A dose of 0.035  
222 mWcm<sup>-2</sup> or B. a dose of 0.076 mWcm<sup>-2</sup> or C. a dose of 0.150 mWcm<sup>-2</sup> or D. a dose of 0.6 mWcm<sup>-2</sup> was applied to irradiate samples  
223 at 405 nm over a course of 24 while sampling at 4, 8, 12 and 24 hours (for A, B and C) or over a course of 8 hours while sampling at  
224 1, 2, 4 and 8 hours (D) was done in independent triplicates. Blue bars indicate treated samples and red bars correspond to the  
225 untreated equivalent that was left at the biosafety cabinet under the same conditions while not subjecting to irradiation. Data shown  
226 as PFU/ml<sup>-1</sup> in triplicate assessed by plaque assay. E. Plaque phenotype comparison from one independent experiment at an  
227 irradiation dose of 0.6 mWcm<sup>-2</sup>. Fixed and blocked plaques were immunostained using anti-NP antibody before developing using  
228 TrueBlue reagent.

229 **Influenza A virus is susceptible to 405 nm inactivation in the absence of**  
230 **photosensitizers.**

231 Given the observations derived from SARS-CoV-2, a separate inactivation study using a  
232 different lipid-enveloped RNA virus was conducted by using influenza A Puerto Rico  
233 (A/H1N1/PR8-Mount Sinai) virus strain. Irradiation with a high dose of  $0.6 \text{ mWcm}^{-2}$   
234 suggested a time dependent reduction of infectivity of 31.11%, 63.33%, 81.56% and  
235 98.49% (66 tiems) at 1, 2, 4 and 8 hours respectively (Figure 3A and 3B).



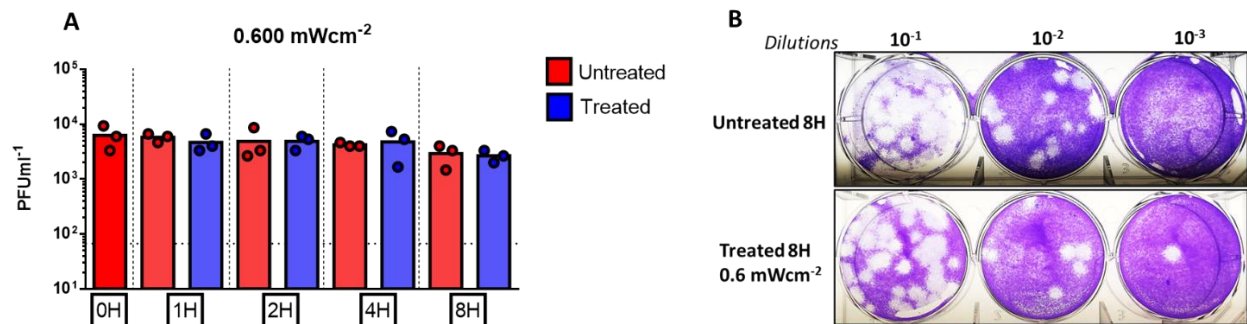
236

237 **Figure 3 Inactivation of Influenza A virus in PBS by 405 nm irradiation. A.** A dose of  $0.6 \text{ mWcm}^{-2}$  was applied to irradiate  
238 samples at 405 nm over a course 8 hours while sampling at 1, 2, 4 and 8 hours (done in independent triplicates). Blue bars indicate  
239 treated samples and red bars correspond to the untreated equivalent that was left at the biosafety cabinet under the same  
240 conditions while not subjecting to irradiation. Data shown as PFU/ml in triplicate assessed by plaque assay. **B.** Plaque phenotype  
241 comparison from one independent experiment at an irradiation dose of  $0.6 \text{ mWcm}^{-2}$ . Fixed and blocked plaques were stained using  
242 crystal violet.

243 The stability of IAV virus at room temperature for a period of 8 hours was found to be  
244 the negligible in untreated IAV spiked PBS samples (Figure 3A).

245 **Encephalomyocarditis virus (EMCV) as a model non-enveloped virus indicates**  
246 **reduced susceptibility to 405 nm inactivation in the absence of photosensitizers.**

247 In order to better understand the effect of the lipid-envelope in viral inactivation by 405  
248 nm irradiation, we used a non-lipid enveloped RNA virus derived from the  
249 *Picornaviridae* family. EMCV virus was irradiated at a high dose of  $0.6 \text{ mWcm}^{-2}$  similar  
250 to SARS-CoV-2 and IAV.



251  
252 **Figure 4. Encephalomyocarditis virus (EMCV) in PBS shows reduced susceptibility to 405 nm irradiation. A.** A dose of  $0.6$   
253  $\text{mWcm}^{-2}$  was applied to irradiate samples at 405 nm over a course 8 hours while sampling at 1, 2, 4 and 8 hours (done in  
254 independent triplicates). Blue bars indicate treated samples and red bars correspond to the untreated equivalent that was left at the  
255 biosafety cabinet under the same conditions while not subjecting to irradiation. Data shown as  $\text{PFUml}^{-1}$  in triplicate assessed by  
256 plaque assay. **B.** Plaque phenotype comparison from one independent experiment at an irradiation dose of  $0.6 \text{ mWcm}^{-2}$ . Fixed and  
257 blocked plaques were stained using crystal violet.

258  
259 In this case however, a total reduction of 9.1% (approximately 2 times) in comparison to  
260 the initial input ( $T_0$ ) after 8 hours of irradiation was observed (Fig 4A and 4 B) indicating  
261 a lower rate of inactivation in contrast to the lipid-enveloped RNA viruses tested in this  
262 study. The plaque reduction at 8 hours did not indicate the same dramatic reduction as  
263 observed with the latter studies.

## 264 Discussion

265 The ongoing SARS-CoV-2 pandemic has affected the day-to-day functions in the entire  
266 world, raising concerns not only with regards to therapeutics but also in the context of

267 virus survivorship and decontamination<sup>35</sup>. Taking into consideration the rapid spread of  
268 SARS-CoV-2 from person to person by droplets, aerosols, and fomites, whole-room  
269 disinfection systems can be viewed as a supplement to best practices for interrupting  
270 transmission of the virus.

271 Given the ongoing COVID-19 pandemic, we wanted to explore the impact of 405 nm  
272 enriched visible light technology on inactivation of respiratory pathogens such as SARS-  
273 CoV-2 and influenza A virus.

274 Without the use of exogenous photosensitizers, we were able to show that irradiation  
275 with low intensity ( $0.035 \text{ mWcm}^{-2}$ ) visible light yielded a total of 55.08% inactivation after  
276 four hours and a total of 90.17% inactivation of SARS-CoV-2 after 24 hours. A slightly  
277 higher dose ( $0.076 \text{ mWcm}^{-2}$ ) resulted in 98.22% inactivation after 24 hours while an  
278 irradiation dose of  $0.150 \text{ mWcm}^{-2}$  showed a reduction of 63.64% and 99.61% after four  
279 hours and 24 hours of irradiation, respectively. Finally, increasing the dose to  $0.6$   
280  $\text{mwcm}^{-2}$  yielded 99.74% after eight hours, indicating a both time and dose dependent  
281 inactivation of infectious viruses. We selected conventional plaque assays as the read  
282 out to specifically estimate infectious virus titers upon disinfection. Methods based in the  
283 quantification of viral RNA via PCR based techniques might be misleading as they  
284 detect viral RNA from both infectious and noninfectious virions.

285 SARS-CoV-2 is a lipid-enveloped virus composed of a ssRNA genome and our data  
286 indicates its susceptibility to visible light mediated inactivation. To further confirm these  
287 observations, we used influenza A virus. which is another human respiratory virus with a  
288 lipid envelop and an RNA genome. Upon irradiating for 1 hour at  $0.6 \text{ mWcm}^{-2}$ , we  
289 observed a total reduction of 31.11% for the influenza A virus compared to the reduction

290 of 71.52% for SARS-CoV-2 under the same conditions. While both viruses have lipid  
291 envelopes, there is clearly a difference here that will require further study. One possible  
292 explanation is the difference in the virion size creating a physically smaller cross-section  
293 for absorption. (IAV ~120 nm and SARS-CoV-2 ~200 nm)<sup>36, 37</sup>. Nevertheless, both  
294 viruses were largely inactivated after eight hours- 98.49% for IAV and 99.74% for  
295 SARS-CoV-2. Intriguingly, it was observed that both RNA viruses were able to remain  
296 stable at room temperature for at least 24 hours, indicating minimal decay which is  
297 consistent with previous studies<sup>35, 38</sup>. We next irradiated a non-enveloped RNA virus,  
298 EMCV. Previous results for visible light against non-enveloped viruses demonstrated  
299 the need for external photosensitizers such as artificial saliva, blood, feces, etc<sup>30, 35</sup>.  
300 Without a porphyrin containing medium, we expected little to no inactivation when this  
301 virus was irradiated with visible light. For these measurements, we used the highest  
302 available irradiance of 0.6 mWcm<sup>-2</sup>. As anticipated, we observed only a 9.1%  
303 inactivation after eight hours, however, this appears to be with the statistical precision of  
304 the measurement based on the results obtained from shorter irradiations (1, 2, and 4  
305 hours). For comparison, a study involving the M13-bacteriophage virus (a non-  
306 enveloped virus) showed a 3-Log reduction using an irradiance of 50mWcm<sup>-2</sup> (almost  
307 100 times greater than the highest irradiance used in this study) for 10 hours at 425 nm  
308 further supporting the idea that non-enveloped viruses may require higher doses of  
309 visible light<sup>39</sup>.

310 Our study was conducted using a neutral liquid media composed of PBS without any  
311 photosensitizers and we were able to show that visible light can indeed inactivate lipid-  
312 enveloped viruses, differing from the theory that states that photosensitizers are a



313 requirement for inactivation. Other studies which used visible light based irradiation  
314 have shown similar results in the absence of photosensitizers, indicating the possibility  
315 of an alternative inactivation mechanism<sup>23, 25, 30</sup>. Studies have proposed two theories for  
316 this observation. The first being that small amounts of 420-430 nm emitted from the  
317 source is contributing to the viral inactivation<sup>40</sup>. This theory most likely doesn't apply  
318 here as the spectrum of light used contains very little irradiance at these wavelengths.  
319 The other theory involves the presence of UV-A (390 nm) created as a byproduct. This  
320 wavelength is known to create oxidative stress upon viral capsids<sup>41</sup>.

321 The results obtained suggest that the performance of visible light against SARS-CoV-2  
322 is similar to organisms commonly found in the environment such as *S. aureus*.  
323 Previous studies have shown that the visible light irradiance levels used in this study  
324 ( $0.035 \text{ mWcm}^{-2}$  to  $0.6 \text{ mWcm}^{-2}$ ) reduce bacteria levels in occupied rooms and improve  
325 outcomes for surgical procedures. It is therefore reasonable to conclude that visible light  
326 might be an effective disinfectant against SARS-CoV-2. More importantly, this  
327 disinfection can operate continuously as it is safe for humans based upon the exposure  
328 guidelines in IEC 62471<sup>42</sup>. This means that once it has been in use for a period of time,  
329 the environment will be cleaner and safer the next time it is occupied by humans.

330 One limitation of this study is that the inactivation assays were performed in static liquid  
331 media as opposed to aerosolized droplets. While the use of visible light in air  
332 disinfection has been briefly studied where it was shown that its effectiveness increased  
333 approximately 4-fold<sup>43</sup>, further studies involving dynamic aerosolization are needed to  
334 better understand the true potential of visible light mediated viral inactivation.

335 In any case, our study shows the increased susceptibility of enveloped respiratory viral  
336 pathogens to 405 nm mediated inactivation in the absence of photosensitizers. The  
337 irradiances used in this study are very low and might be easily applied to safely and  
338 continuously disinfect occupied areas within hospitals, schools, restaurants, offices and  
339 other locations.

## 340 **Acknowledgments**

341 We thank Randy Albrecht for support with the BSL3 facility and procedures at the ISMMS, and  
342 Richard Cadagan for technical assistance. This research was partly funded by CRIP (Center for  
343 Research for Influenza Pathogenesis), a NIAID supported Center of Excellence for Influenza  
344 Research and Surveillance (CEIRS, contract # HHSN272201400008C); by the generous  
345 support of the JPB Foundation, the Open Philanthropy Project (research grant 2020-215611  
346 (5384)) and anonymous donors to AG-S, and by a research contract from Kenall Manufacturing  
347 to the AG-S lab.

## 348 **Conflicts of interest**

349 The García-Sastre Laboratory has received research support from Pfizer, Senhwa  
350 Biosciences, 7Hills Pharma, Avimex, Blade Therapeutics, Dynavax, ImmunityBio,  
351 Nanocomposix and Kenall Manufacturing. Adolfo García-Sastre has consulting  
352 agreements for the following companies involving cash and/or stock: Vivaldi  
353 Biosciences, Pagoda, Contrafect, 7Hills Pharma, Avimex, Vaxalto, Accurius, Pfizer and  
354 Esperovax. RR, CY and AGS have filed for a provisional patent based upon these  
355 results.

## 356 **References**

- 357 1. Andersen, K. G., Rambaut, A., Lipkin, W. I., Holmes, E. C. & Garry, R. F. The  
358 proximal origin of SARS-CoV-2. *Nat. Med.* **26**, 450-452 (2020).
- 359 2. Worldometer, D. COVID-19 coronavirus pandemic. *World Health Organization*,  
360 [www.worldometers.info](http://www.worldometers.info) (2020).
- 361 3. Buitrago-Garcia, D. *et al.* Occurrence and transmission potential of asymptomatic and  
362 presymptomatic SARS-CoV-2 infections: A living systematic review and meta-analysis.  
363 *PLoS medicine* **17**, e1003346 (2020).
- 364 4. [https://www.who.int/news-room/commentaries/detail/modes-of-transmission-of-virus-](https://www.who.int/news-room/commentaries/detail/modes-of-transmission-of-virus-causing-covid-19-implications-for-ipc-precaution-recommendations)  
365 [causing-covid-19-implications-for-ipc-precaution-recommendations](https://www.who.int/news-room/commentaries/detail/modes-of-transmission-of-virus-causing-covid-19-implications-for-ipc-precaution-recommendations).
- 366 5. Dehbandi, R. & Zazouli, M. A. Stability of SARS-CoV-2 in different environmental  
367 conditions. *The Lancet Microbe* **1**, e145 (2020).
- 368 6. Van Doremalen, N. *et al.* Aerosol and surface stability of SARS-CoV-2 as compared  
369 with SARS-CoV-1. *N. Engl. J. Med.* **382**, 1564-1567 (2020).
- 370 7. Behzadinasab, S., Chin, A., Hosseini, M., Poon, L. & Ducker, W. A. A surface coating  
371 that rapidly inactivates SARS-CoV-2. *ACS applied materials & interfaces* **12**, 34723-  
372 34727 (2020).
- 373 8. Chan, K. *et al.* Factors affecting stability and infectivity of SARS-CoV-2. *J. Hosp.*  
374 *Infect.* **106**, 226-231 (2020).
- 375 9. Biryukov, J. *et al.* Increasing Temperature and Relative Humidity Accelerates  
376 Inactivation of SARS-CoV-2 on Surfaces. *mSphere* **5**, 10.1128/mSphere.00441-20  
377 (2020).
- 378 10. Aboubakr, H. A., Sharafeldin, T. A. & Goyal, S. M. Stability of SARS-CoV-2 and  
379 other coronaviruses in the environment and on common touch surfaces and the  
380 influence of climatic conditions: A review. *Transboundary and emerging diseases*  
381 (2020).
- 382 11. Smither, S. J., Eastaugh, L. S., Findlay, J. S. & Lever, M. S. Experimental aerosol  
383 survival of SARS-CoV-2 in artificial saliva and tissue culture media at medium and high  
384 humidity. *Emerging microbes & infections* **9**, 1415-1417 (2020).
- 385 12. Schuit, M. *et al.* Airborne SARS-CoV-2 is rapidly inactivated by simulated sunlight.  
386 *J. Infect. Dis.* **222**, 564-571 (2020).
- 387 13. Kampf, G., Todt, D., Pfaender, S. & Steinmann, E. Persistence of coronaviruses on  
388 inanimate surfaces and their inactivation with biocidal agents. *J. Hosp. Infect.* **104**, 246-  
389 251 (2020).

- 390 14. Rutala, W. A. & Weber, D. J. Disinfection and sterilization in health care facilities:  
391 what clinicians need to know. *Clinical infectious diseases* **39**, 702-709 (2004).
- 392 15. Rathnasinghe, R. *et al.* Scalable, effective, and rapid decontamination of SARS-  
393 CoV-2 contaminated N95 respirators using germicidal ultra-violet C (UVC) irradiation  
394 device. *medRxiv* (2020).
- 395 16. Escombe, A. R. *et al.* Upper-room ultraviolet light and negative air ionization to  
396 prevent tuberculosis transmission. *PLoS Med* **6**, e1000043 (2009).
- 397 17. Nakpan, W., Yermakov, M., Indugula, R., Reponen, T. & Grinshpun, S. A.  
398 Inactivation of bacterial and fungal spores by UV irradiation and gaseous iodine  
399 treatment applied to air handling filters. *Sci. Total Environ.* **671**, 59-65 (2019).
- 400 18. Tseng, C. & Li, C. Inactivation of viruses on surfaces by ultraviolet germicidal  
401 irradiation. *Journal of occupational and environmental hygiene* **4**, 400-405 (2007).
- 402 19. Kowalski, W. in *Ultraviolet germicidal irradiation handbook: UVGI for air and surface*  
403 *disinfection* (Springer science & business media, 2010).
- 404 20. Zaffina, S. *et al.* Accidental exposure to UV radiation produced by germicidal lamp:  
405 case report and risk assessment. *Photochem. Photobiol.* **88**, 1001-1004 (2012).
- 406 21. Leung, K. C. P. & Ko, T. C. S. Improper Use of the Germicidal Range Ultraviolet  
407 Lamp for Household Disinfection Leading to Phototoxicity in COVID-19 Suspects.  
408 *Cornea* **40**, 121-122 (2021).
- 409 22. Maclean, M. *et al.* Environmental decontamination of a hospital isolation room using  
410 high-intensity narrow-spectrum light. *J. Hosp. Infect.* **76**, 247-251 (2010).
- 411 23. Maclean, M., McKenzie, K., Anderson, J. G., Gettinby, G. & MacGregor, S. J. 405  
412 nm light technology for the inactivation of pathogens and its potential role for  
413 environmental disinfection and infection control. *J. Hosp. Infect.* **88**, 1-11 (2014).
- 414 24. Murrell, L. J., Hamilton, E. K., Johnson, H. B. & Spencer, M. Influence of a visible-  
415 light continuous environmental disinfection system on microbial contamination and  
416 surgical site infections in an orthopedic operating room. *Am. J. Infect. Control* **47**, 804-  
417 810 (2019).
- 418 25. Maclean, M., Murdoch, L. E., MacGregor, S. J. & Anderson, J. G. Sporicidal effects  
419 of high-intensity 405 nm visible light on endospore-forming bacteria. *Photochem.*  
420 *Photobiol.* **89**, 120-126 (2013).
- 421 26. Murdoch, L., McKenzie, K., Maclean, M., Macgregor, S. & Anderson, J. Lethal  
422 effects of high-intensity violet 405-nm light on *Saccharomyces cerevisiae*, *Candida*

- 423 albicans, and on dormant and germinating spores of *Aspergillus niger*. *Fungal Biology*  
424 **117**, 519-527 (2013).
- 425 27. Dai, T. *et al.* Blue light for infectious diseases: *Propionibacterium acnes*,  
426 *Helicobacter pylori*, and beyond? *Drug Resistance Updates* **15**, 223-236 (2012).
- 427 28. Bumah, V. V. *et al.* Spectrally resolved infrared microscopy and chemometric tools  
428 to reveal the interaction between blue light (470 nm) and methicillin-resistant  
429 *Staphylococcus aureus*. *Journal of Photochemistry and Photobiology B: Biology* **167**,  
430 150-157 (2017).
- 431 29. Hadi, J., Dunowska, M., Wu, S. & Brightwell, G. Control Measures for SARS-CoV-2:  
432 A Review on Light-Based Inactivation of Single-Stranded RNA Viruses. *Pathogens* **9**,  
433 737 (2020).
- 434 30. Tomb, R. M. *et al.* New proof-of-concept in viral inactivation: virucidal efficacy of 405  
435 nm light against feline calicivirus as a model for norovirus decontamination. *Food and*  
436 *environmental virology* **9**, 159-167 (2017).
- 437 31. Ho, D. T. *et al.* Effect of blue light emitting diode on viral hemorrhagic septicemia in  
438 olive flounder (*Paralichthys olivaceus*). *Aquaculture* **521**, 735019 (2020).
- 439 32. Wu, J. *et al.* Virucidal efficacy of treatment with photodynamically activated  
440 curcumin on murine norovirus bio-accumulated in oysters. *Photodiagnosis and*  
441 *photodynamic therapy* **12**, 385-392 (2015).
- 442 33. Martinez-Sobrido, L. & Garcia-Sastre, A. Generation of recombinant influenza virus  
443 from plasmid DNA. *J. Vis. Exp.* **(42)**. pii: 2057. doi, 10.3791/2057 (2010).
- 444 34. Carocci, M. & Bakkali-Kassimi, L. The encephalomyocarditis virus. *Virulence* **3**, 351-  
445 367 (2012).
- 446 35. Derraik, J. G., Anderson, W. A., Connelly, E. A. & Anderson, Y. C. Rapid evidence  
447 summary on SARS-CoV-2 survivorship and disinfection, and a reusable PPE protocol  
448 using a double-hit process. *MedRxiv* (2020).
- 449 36. Bouvier, N. M. & Palese, P. The biology of influenza viruses. *Vaccine* **26**, D49-D53  
450 (2008).
- 451 37. Bar-On, Y. M., Flamholz, A., Phillips, R. & Milo, R. Science Forum: SARS-CoV-2  
452 (COVID-19) by the numbers. *Elife* **9**, e57309 (2020).
- 453 38. Wang, X., Zoueva, O., Zhao, J., Ye, Z. & Hewlett, I. Stability and infectivity of novel  
454 pandemic influenza A (H1N1) virus in blood-derived matrices under different storage  
455 conditions. *BMC infectious diseases* **11**, 1-6 (2011).

- 456 39. Tomb, R. M. *et al.* Inactivation of *Streptomyces* phage  $\phi$ C31 by 405 nm light:  
457 Requirement for exogenous photosensitizers? *Bacteriophage* **4**, e32129 (2014).
- 458 40. Richardson, T. B. & Porter, C. D. Inactivation of murine leukaemia virus by exposure  
459 to visible light. *Virology* **341**, 321-329 (2005).
- 460 41. Girard, P. *et al.* *UVA-induced damage to DNA and proteins: direct versus indirect*  
461 *photochemical processes* (Journal of Physics: Conference Series Ser. 261, IOP  
462 Publishing, 2011).
- 463 42. IEC 62471: Photobiological safety of lamps and lamp systems. (2006).
- 464 43. Dougall, L. R., Anderson, J. G., Timoshkin, I. V., MacGregor, S. J. & Maclean, M.  
465 *Efficacy of antimicrobial 405 nm blue-light for inactivation of airborne bacteria* (Light-  
466 Based Diagnosis and Treatment of Infectious Diseases Ser. 10479, International  
467 Society for Optics and Photonics, 2018).
- 468 44. Nardell, E. A. *et al.* Safety of upper-room ultraviolet germicidal air disinfection for  
469 room occupants: results from the Tuberculosis Ultraviolet Shelter Study. *Public Health*  
470 *Rep.* **123**, 52-60 (2008).
- 471
- 472
- 473